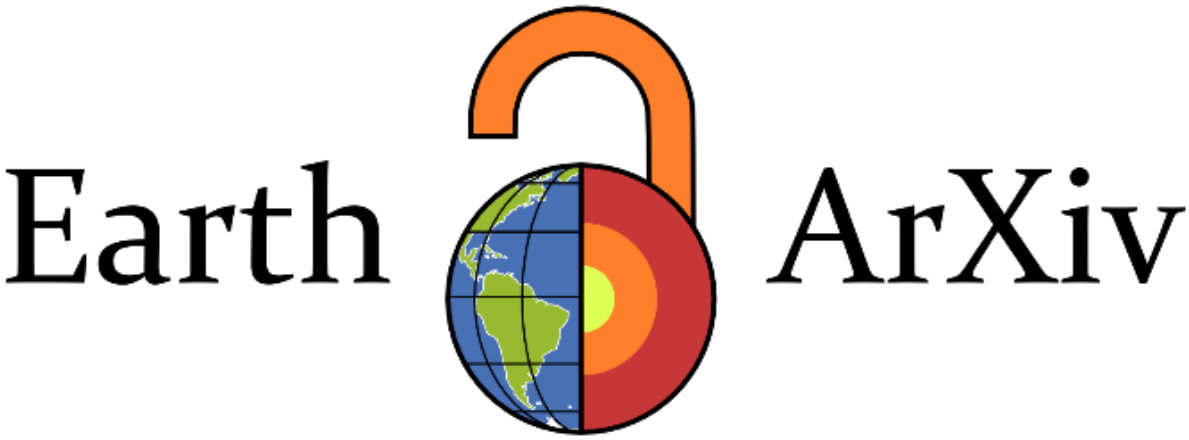

EarthArXiv Preprint

This manuscript is a non-peer-reviewed preprint submitted to EarthArXiv.

Subsequent versions may have different content.

Submitted to EarthArXiv: May 6, 2026

Author ORCID iDs:

Abhilash M Bairy	https://orcid.org/0009-0008-5814-3916
Arjit Praveen	https://orcid.org/0009-0002-0920-6163
Charuvi L S	https://orcid.org/0009-0005-6078-0875
Deeksha Sudheer	https://orcid.org/0009-0008-4750-531X

Comparative Machine Learning approach to seasonal ENSO Forecasting with Time-Series Performance Evaluation

Abhilash M Bairy[1], Arjit Praveen[2], Charuvi L S[3], Deeksha Sudheer[4]
Department of Computer Science and Engineering
BMS Institute of Technology and Management, Bengaluru, India
[1]1by23cs005@bmsit.in, [2]1by23cs030@bmsit.in, [3]1by23cs048@bmsit.in, [4]1by23cs054@bmsit.in

***Abstract*—The El Niño-Southern Oscillation (ENSO) is one of the most important climate phenomena that affects weather conditions worldwide. It influences monsoon seasons, droughts, and crop productivity. Forecasting of ENSO processes is rather difficult since the system is inherently nonlinear. Moreover, the Spring Predictability Barrier limits the predictive capacity of forecasters during the boreal spring period.**

In this paper, four machine learning algorithms – Ridge Regression, Support Vector Regression (SVR), Random Forest, and Long Short-Term Memory (LSTM) are considered. Training was performed on the historical data of the Niño 3.4 and Oceanic Niño Index indices collected over decades. The quality of predictions was evaluated using several lead times from 1 to 15 months with RMSE, MAE, and Pearson correlation coefficient being utilized as metrics.

This paper evaluates and compares the abilities of four machine learning methods in predicting ENSO processes. Although simpler methods give relatively good forecasts on a short term, LSTM shows better results with a longer horizon due to its ability to temporal dependencies. Besides, the influence of the Spring Predictability Barrier on the predictability of ENSO events is evaluated.

***Index Terms*—ENSO, El Niño, La Niña, Machine Learning, Time-Series Forecasting, LSTM, Random Forest, Support Vector Regression, Ridge Regression, Spring Predictability Barrier, Climate Prediction**

I. Introduction

The El Niño-Southern Oscillation (ENSO) is one of the key climate phenomena impacting the entire globe [1], [11]. ENSO causes changes in sea surface temperatures (SSTs) and affects many climatic phenomena such as monsoon, droughts, and agricultural activity [12]. Due to its widespread influence on different climatic parameters, forecasting ENSO is crucial for efficient disaster management, planning, and economy in general [13].

Traditionally, forecasting ENSO used dynamical climate models that simulate complex interactions between atmosphere and oceans [3], [14]. The results obtained by means of the approach mentioned above are impressive yet they demand huge amount of computational power and usually lack long-term forecasts [15]. The main issue associated with traditional forecasting is a so-called Spring Predictability Barrier (SPB) [10]. During SPB, the forecast becomes less accurate since the ocean-atmosphere interaction decreases [10].

Over the last decades [6], machine learning (ML) has become an effective tool to address time series forecasting tasks [18]. Unlike traditional dynamical models, ML algorithms do not need complex physics-based models since they automatically capture complex nonlinear relations using historical data [5]. Ridge Regression, Support Vector Regression (SVR), Random Forest, and LSTM neural network have proven their effectiveness in predicting ENSO accurately [9], [19], [20].

In this study, a comparative analysis of these four machine learning models is performed using historical Niño 3.4 and Oceanic Niño Index (ONI) datasets [6] . The models are evaluated across multiple lead times ranging from 1 to 15 months using performance metrics such as Root Mean Square Error (RMSE), Mean Absolute Error (MAE), and Pearson correlation coefficient [7], [8].

The central purpose of this study is to investigate the efficiency of various machine learning methods used in the ENSO forecast as well as the influence of the Spring Predictability Barrier, finding out the limitations of reliable forecast [10].

II. Related Work

ENSO forecasts employ dynamical methods, statistical techniques, and machine learning algorithms [16]. This part of the literature review highlights scientific papers which are relevant for the current research.

A. Statistical and Traditional Machine Learning Approaches

The first approaches were built upon the use of linear regression, Markov-chains, and EOF decomposition methods [25], [27]. The Linear Inverse Model (LIM) [27] describes the behavior of tropical Pacific SSTA [27]in a way that can be viewed as stochastic forcing of a linear system, which exhibits a similar performance [33]–[35] to numerical models [35]. Lartey Quayesam et al. [28] investigated four machine learning techniques such as LASSO, Ridge, Random Forest, and XGBoost to make predictions of SSTA. All tree-based algorithms outperformed their linear counterparts in all metrics, with XGBoost producing the lowest KLD value (0.018) [19], [29].

B. Deep Learning for ENSO Forecasting

Ham et al. [30] showed a CNN trained on CMIP5 simulations via transfer learning could predict the Niño 3.4 index with $r = 0.5$ up to 17 months ahead, establishing transfer learning as a standard paradigm for ENSO forecasting. Wang et al. [31] extended this with the STIEF model — combining CNN, ResNet, and Temporal Convolutional Network branches — achieving effective skill [30]–[32] to 22 months. Saha and Nanjundiah [32] used an autoencoder for unsupervised feature learning from seven climatic variables, predicting the Niño 3.4 index with $r = 0.87$ at 1-month lead, with nonlinear feature selection outperforming linear correlation alone.

C. Explainability and Hybrid Approaches

Gan et al. [33] introduced the PPTV interpretability framework, confirming that ENSO predictability originates from the tropical Pacific at short leads, with Indian and Atlantic Ocean contributions growing at longer leads — and that the Spring Predictability Barrier may reflect an insufficiency in the input variable set rather than a structural model failure. Feng et al. [34] integrated a ConvLSTM residual correction into the LDEO5 dynamical model, achieving skill to 20 months without requiring CMIP simulations. Schloer et al. [35] proposed a LIM-LSTM hybrid that reaches 12-month ACC above 0.5 with only 50–100 years of training data — far less than the 300 years required by a standalone LSTM — while also capturing asymmetric El Niño/La Niña evolution absent in linear models.

D. Positioning of the Present Work

Unlike approaches relying on large climate simulations [30], [31], [35] or hybrid architectures [34], this study directly compares four practically accessible models — Ridge Regression, SVR, Random Forest, and LSTM — trained exclusively on observational records (1982–2026). This allows explicit quantification of the complexity–skill trade-off, analysis of the Spring Predictability Barrier at each lead time, and identification of conditions under which regularised linear models remain competitive — findings consistent with the broader literature [28], [35].

III. Proposed Methodology

We develop a multi-model approach to predict the Niño 3.4 index, evaluating four regression models — Ridge Regression, SVR, Random Forest, and LSTM — using the same data, features, and evaluation criteria.

A. Problem Formulation

Let $\mathbf{x}_t \in \mathbb{R}^4$ denote multivariate climate observations at time t: Niño 3.4 SST anomaly, Southern Oscillation Index (SOI), OLR anomaly, and Indian Ocean SST. The goal is to learn:

$$f_\tau : \mathbf{X}_t \longrightarrow y_{t+\tau}, \qquad \tau \in \{1,\ 3,\ 6,\ 9,\ 12,\ 15\},$$

where $\mathbf{X}_t$ is the structured representation of the previous six months' observations [7], [8] .

B. Data Sources

Four time series are merged via outer join and ordered chronologically: (1) **Niño 3.4 index** — SST anomaly from NOAA for the Niño 3.4 region (5°N–5°S, 170°W–120°W); (2) **SOI** — standardised sea-level pressure difference (Tahiti minus Darwin); (3) **OLR** — outgoing longwave radiation anomaly ($\mathrm{W\,m^{-2}}$); and (4) **Indian Ocean SST** [6].

C. Feature Engineering

Flat Lag Vector (Ridge / SVR / Random Forest): A flat feature vector is constructed using lags $\ell \in \{1, \ldots, 6\}$ of all four variables:

$$\mathbf{X}_t^{\text{flat}} = \left[\, x_{t-1}^{(1)}, \ldots, x_{t-6}^{(1)},\ x_{t-1}^{(2)}, \ldots, x_{t-1}^{(4)}, \ldots, x_{t-6}^{(4)} \,\right] \in \mathbb{R}^{24},$$

with variable ordering (`nino34`, `soi`, `olr`, `sst_india`). The target is $y = \texttt{nino34}_{t+\tau}$. Rows containing `NaN` are dropped before splitting [5].

Sequence Tensor (LSTM): The lag window is reshaped into a chronologically ordered tensor:

$$\mathbf{X}_t^{\text{3D}} = \left[\, \mathbf{x}_{t-6},\ \ldots,\ \mathbf{x}_{t-1} \,\right] \in \mathbb{R}^{6\times 4}.$$

D. Train–Test Split

Strictly chronological partitioning with no temporal shuffle:

$$\mathcal{D}_{\text{train}} = \left[\, t_1,\ t_{\lfloor 0.8N \rfloor} \,\right], \qquad \mathcal{D}_{\text{test}} = \left[\, t_{\lfloor 0.8N \rfloor + 1},\ t_N \,\right],$$

with N the number of samples after `NaN`-filtering (80% train, 20% test) [7].

E. Model Specifications

A. Ridge Regression:

$$\hat{\boldsymbol{\beta}} = \arg\min_{\boldsymbol{\beta}} \left\| \mathbf{X}^{\text{flat}}\boldsymbol{\beta} - \mathbf{y} \right\|_2^2 + \alpha \left\|\boldsymbol{\beta}\right\|_2^2, \qquad \alpha = 1.0.$$

Inputs standardised via `StandardScaler` fitted on training set only [26]

B. Support Vector Regression: SVR with RBF kernel $k(\mathbf{x}_i, \mathbf{x}_j) = \exp\!\left(-\gamma \|\mathbf{x}_i - \mathbf{x}_j\|^2\right)$ solves the ε-insensitive regression problem. Hyperparameters tuned per lead time by 5-fold `TimeSeriesSplit` grid search over $C \in \{0.1, 1, 10\}$ and $\varepsilon \in \{0.01, 0.1\}$. Inputs standardised identically to Ridge [26].

C. Random Forest:

$$\hat{y} = \frac{1}{T} \sum_{t=1}^{T} h_t\!\left(\mathbf{X}^{\text{flat}}\right),$$

[9]with each tree grown on a bootstrap sample using a random feature subset. No feature scaling applied. Hyperparameters tuned per lead via grid search: $T \in \{100, 200\}$, $d_{\max} \in \{5, 10, \text{None}\}$, $m_{\text{feat}} \in \{\sqrt{p},\ 0.5p\}$, `random_state=42`.

D. LSTM Network: Input $\mathbf{X}^{\text{3D}} \in \mathbb{R}^{6\times 4}$, channel-wise standardised. Architecture: (1) two stacked LSTM layers (hidden size 64, dropout 0.2); (2) dropout 0.2 on final hidden state $\mathbf{h}_6$; (3) FC layer: $\mathbf{z} = \text{ReLU}(\mathbf{W}_1\mathbf{h}_6 + \mathbf{b}_1) \in \mathbb{R}^{32}$; (4) output: $\hat{y} = \mathbf{W}_2\mathbf{z} + b_2$.

Training: Adam (lr $= 10^{-3}$, weight decay 10^{-4}), MSE loss, gradient clipping ($\|\mathbf{g}\|_2 \le 1.0$), `ReduceLROnPlateau` (factor 0.5, patience 10), early stopping (patience 20, best-weight restore), max 150 epochs, batch size 32, `random_state=42`.

F. Evaluation Metrics

Models are evaluated on the held-out test set using:

$$\text{RMSE} = \sqrt{\frac{1}{n}\sum_{i=1}^{n}(y_i - \hat{y}_i)^2} \tag{1}$$

$$\text{MAE} = \frac{1}{n}\sum_{i=1}^{n}|y_i - \hat{y}_i| \tag{2}$$

$$r = \frac{\sum_{i=1}^{n}(y_i - \bar{y})(\hat{y}_i - \bar{\hat{y}})}{\sqrt{\sum_{i=1}^{n}(y_i - \bar{y})^2 \ \sum_{i=1}^{n}(\hat{y}_i - \bar{\hat{y}})^2}} \tag{3}$$

F. Outputs and Comparison

Results are presented via interactive `plotly` visualisations: RMSE and MAE vs. lead time; Pearson-r skill decay curve ($r = 0.6$ marked); RMSE heatmap (model vs. lead time); Niño 3.4 predicted vs. observed plots with El Niño ($\geq +0.5$°C) and La Niña (≤ -0.5°C) phases highlighted; LSTM training/validation loss curves; and Random Forest feature importance heatmap.

IV. System Implementation

This work presents a machine learning approach to predicting the Niño 3.4 index to forecast El Niño-Southern Oscillation (ENSO) [18]. The approach relies on an implemented pipeline including data gathering, preprocessing, feature engineering, modeling, and testing of a chosen algorithm to predict the sea surface temperature anomalies at different time lags.

A. Development Environment

Python language is used as the main programming environment because of extensive support in scientific computing and machine learning areas provided by several libraries [21] . NumPy and Pandas provide functionality for performing calculations with multidimensional arrays and manipulating with data, respectively [22]. SciPy can be used for statistical computation, and Plotly for visualizations. Scikit-learn is used for constructing classical machine learning algorithms, while PyTorch for deep learning models like LSTM [9], [23].

B. Data Acquisition

The dataset includes the monthly data for both Niño 3.4 index and Oceanic Niño Index (ONI) collected from NOAA [6]. The period covered by data starts from 1950 up to current date and represents the SST anomalies in the equatorial Pacific Ocean.

C. Data Preprocessing

The following tasks are done for preprocessing the data:

- Missing values interpolation
- Normalizing SST anomalies for better training consistency
- Maintaining time sequence to prevent any data leakage

D. Feature Engineering

Lag-based features are created to capture dependency on time. Past 12 months SST anomalies ($t-1$ to $t-12$) are considered as input features for forecasting future SST anomalies.

E. Train-Test Split

A strict time-based split is used:

- Training set: 1950–2005
- Testing set: 2006–Present

This approach ensures realistic forecasting conditions.

F. Model Implementation

Four models are implemented:

- Ridge Regression (linear baseline)
- Support Vector Regression (SVR)
- Random Forest (ensemble learning)
- Long Short-Term Memory (LSTM)

G. Training Strategy

Each model is trained independently for multiple lead times (1, 3, 6, 9, 12, and 15 months). Hyperparameters are tuned using validation data to achieve optimal performance [7].

H. Evaluation Metrics

The models are evaluated using:

- Root Mean Square Error (RMSE)
- Mean Absolute Error (MAE)
- Pearson Correlation Coefficient (r)

[8]

I. Baseline Comparison

A persistence model is used as a baseline, where future values are assumed to be equal to current observations.

J. Workflow Description

The workflow of the system is described below:

1) SST anomaly data acquisition from NOAA datasets
2) Data preprocessing by normalizing and addressing missing values
3) Creation of time-lagged features
4) Temporal split to train and test datasets
5) Training machine learning models for different forecast lead times
6) Prediction of SST anomalies for future periods
7) Evaluation of performance using RMSE, MAE, and correlation coefficient
8) Comparison across models and lead times

This approach allows for replicability and scalability for various forecast lead times [2].

V. Results

In addition to previous evaluations, four methods, namely, Ridge regression, Support Vector Regression (SVR), Random Forest and LSTM, are compared for forecasting of Niño 3.4 index at lead time from 1 to 15 months [9], [19], [20], utilizing a sequential 80:20 split based on the number of 531 samples from January 1982 to March 2026. [2] Forecast performance metrics include Root Mean Squared Error (RMSE) (in °C) and Pearson correlation coefficient (r) where $r \geq 0.6$ indicates a skillful forecast [2].

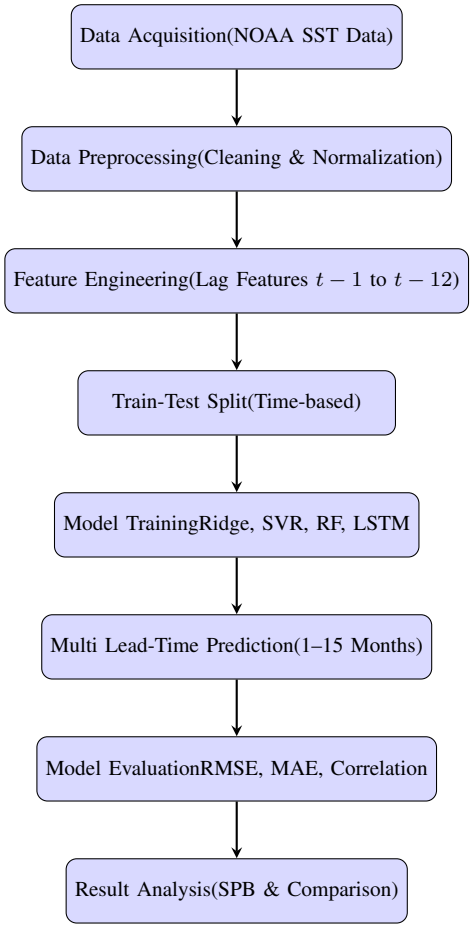

Fig. 1. End-to-End ENSO Forecasting Pipeline

A. Comparative Performance

The full results are presented in Table I. Skill decreases with increasing lead time across all models due to the spring predictability barrier effect [10] [4].

TABLE I
TEST-SET RMSE (°C) AND PEARSON r FOR ALL MODELS AND LEAD TIMES. BOLD = BEST PER LEAD.

Lead	Ridge		SVR		Random Forest		LSTM	
	RMSE	r	RMSE	r	RMSE	r	RMSE	r
1 m	0.3563	0.8951	0.3167	0.9145	0.3113	0.9182	**0.2822**	**0.9403**
3 m	0.5278	0.7594	0.4727	0.7949	0.4592	0.8093	**0.4549**	**0.8423**
6 m	0.7078	0.4453	**0.6938**	**0.4588**	0.7161	0.3925	0.7208	0.4097
9 m	**0.7540**	**0.2669**	0.8528	−0.3064	0.8535	−0.1436	0.7958	−0.2358
12 m	**0.7508**	**0.4669**	0.8438	−0.3221	0.8731	−0.2118	0.7907	−0.3972
15 m	**0.7422**	**0.3871**	0.8024	−0.1445	0.8830	−0.2159	0.7569	0.2695

B. Short- and Medium-Range Skill (Leads 1–6 Months)

All models surpass the skill threshold at the 1-month lead. LSTM is again the best performing one ($r = 0.9403$, RMSE $= 0.2822$°C) followed by RF ($r = 0.9182$), SVR ($r = 0.9145$) and Ridge ($r = 0.8951$). The order of models does not change at 3 months lead, with all models showing correlation above $r = 0.6$. Such an order at short leads is due to the ability of LSTM to capture non-linear temporal dependencies within the 6 months period of the time window [30].

SVR outperforms other methods at 6-months lead, the seasonality predictability threshold [2], providing the minimum RMSE (0.6938°C, $r = 0.4588$), which is only slightly higher than that for Ridge. At this lead, the performance gap disappears, and the most complex models, namely LSTM and Random Forest, do not demonstrate any advantage anymore, since stronger regularization performed by Ridge and SVR allows suppressing noise [20].

Fig. 2. Pearson r vs. lead time. Dashed orange line marks the $r = 0.6$ skill threshold. Ridge is the only model retaining positive correlation at all leads.

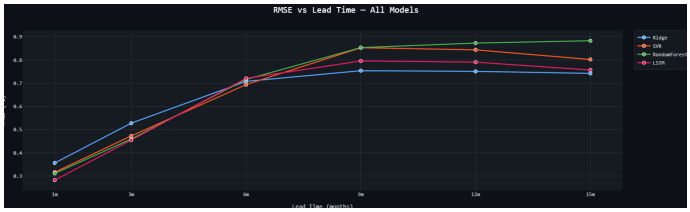

Fig. 3. RMSE (°C) vs. lead time. Ridge degrades gradually; SVR and Random Forest degrade sharply beyond 6 months.

C. Long-Range Skill (Leads 9–15 Months)

After the 6-month point, another important difference becomes apparent. The Ridge approach remains positively correlated at all lead times, which is not the case for the remaining approaches: SVR, Random Forest, and LSTM yield *negative* correlations at both 9 and 12 months that are even less than those of climatology, meaning they are over-fitted by the medium range signal. The L_2 penalty of the Ridge model brings the weights closer to zero in absence of signal, resulting in close-to-climatology prediction and reduced RMSE (0.75–0.76°C versus 0.79–0.88°C) [5].

It should be noted that the RMS of Ridge at the 12-month lead time is smaller (0.7508°C) than at 9 months, probably because of its partial capture of ENSO periodicity. The LSTM model partially returns to form at 15 months ($r = 0.2695$) [19].

D. Individual Model Description

Ridge Regression employs 24 standardized predictors (4 variables × 6 lags), $\alpha = 1.0$. From coefficient importance analysis, we find that short-lagged Niño 3.4 predictors have

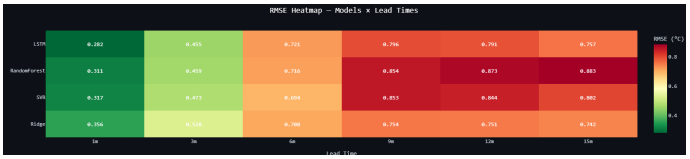

Fig. 4. RMSE heatmap across all model–lead combinations. Greener = lower error. Ridge's stability at long leads is clearly visible.

significant influence at lead 1, whereas SOI and Indian Ocean SST lags become important for longer leads, in agreement with the thermocline recharge mechanism [17] .

Support Vector Regression (SVR) with RBF kernel and optimal parameters tuned using 5-fold `TimeSeriesSplit` starts with $C = 1$, $\varepsilon = 0.01$ at short leads and ends up with $C = 0.1$, $\varepsilon = 0.1$ at longer leads. It reaches maximum performance at a lead time of 6 months, where moderate nonlinearity provides a slight edge over Ridge regression.

Random Forest works well with short leads but has the largest RMSE among the models at 9-15 month leads. Importance values of features validate the dominating role of short-lag Niño 3.4 with additional importance of Indian Ocean SSTs at 6-12 months leads [26].

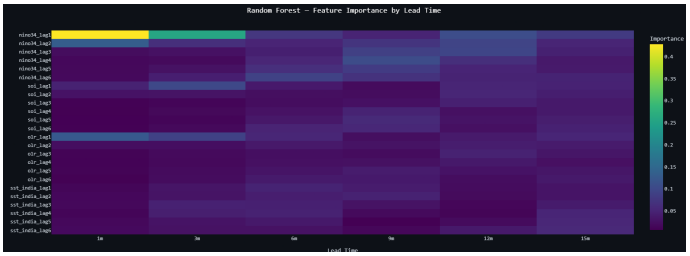

Fig. 5. Random Forest feature importance heatmap. Short-lag Niño 3.4 features dominate; Indian Ocean SST gains importance at 6–12-month leads.

LSTM (model with two stacked LSTM layers with 64 hidden units, dropout = 0.2; input shape of $(N, 6, 4)$) is easy to converge at short leads (early stopping after epoch 35 for lead = 1), whereas for leads between 9-12, early stopping happens at epoch 22-26, with divergence in train/validation loss.

E. Predicted vs. Observed Anomalies

Figures 7 to 8 display the comparison between the predicted and observed values for Niño 3.4 based on the test data. The main qualitative results include the following: the start of the El Niño event was reasonably well predicted up to 1-3 months ahead (including the super El Niño in 2015–2016); the depth of La Niña was consistently underestimated for lead times greater than 3 months; phase inversions were found in SVR and Random Forest for 9-15 months ahead, whereas Ridge and LSTM

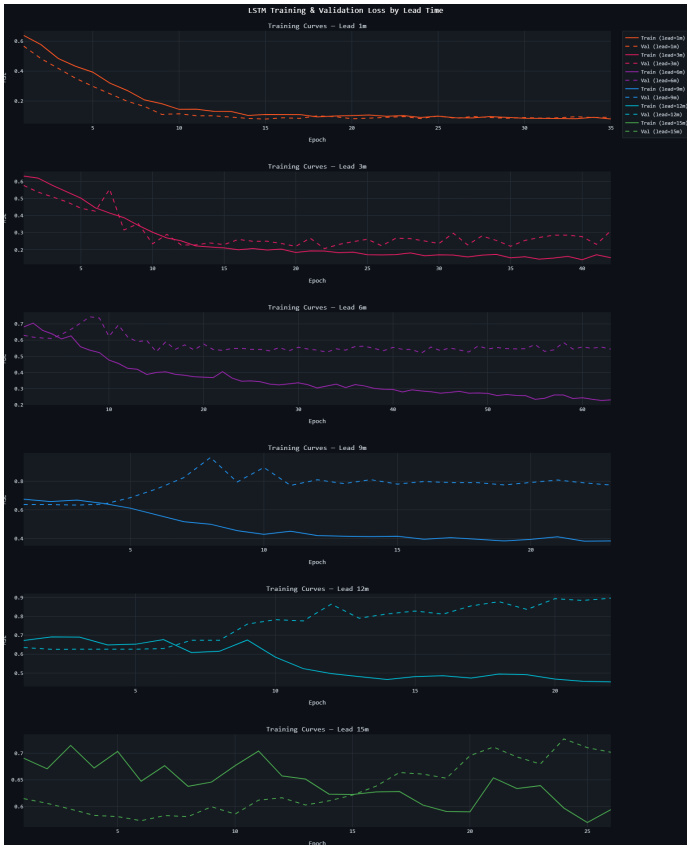

Fig. 6. LSTM train/validation MSE curves. Short leads converge smoothly; long leads show diverging trajectories and early stopping at epochs 22–26.

F. Summary

1) **LSTM dominates from 1-3 months**, with an RMSE performance gain ranging from 5-14% compared to Ridge due to its superior encoding scheme based on sequential temporality.
2) **Support Vector Regression (SVR) dominates from 6 months** (RMSE = 0.6938°C), emerging as the optimal choice for the spring-barrier prediction horizon.
3) **Ridge is the sole consistent model from 6 months onwards**, sustaining a positive correlation coefficient across all leads, whereas other models exhibit a drop to negative values.
4) **None of the models outperform** $r = 0.50$ **from 9 months onwards**, reaffirming the inherent limit of ENSO predictability.

VI. Discussion

Key learnings from the experimental findings include the following:

A. Model Predictive Capability

Firstly, the experiment shows that all models have high accuracy in their predictions at short lead times (1–3 months) owing to high correlation values and minimal error rates. This

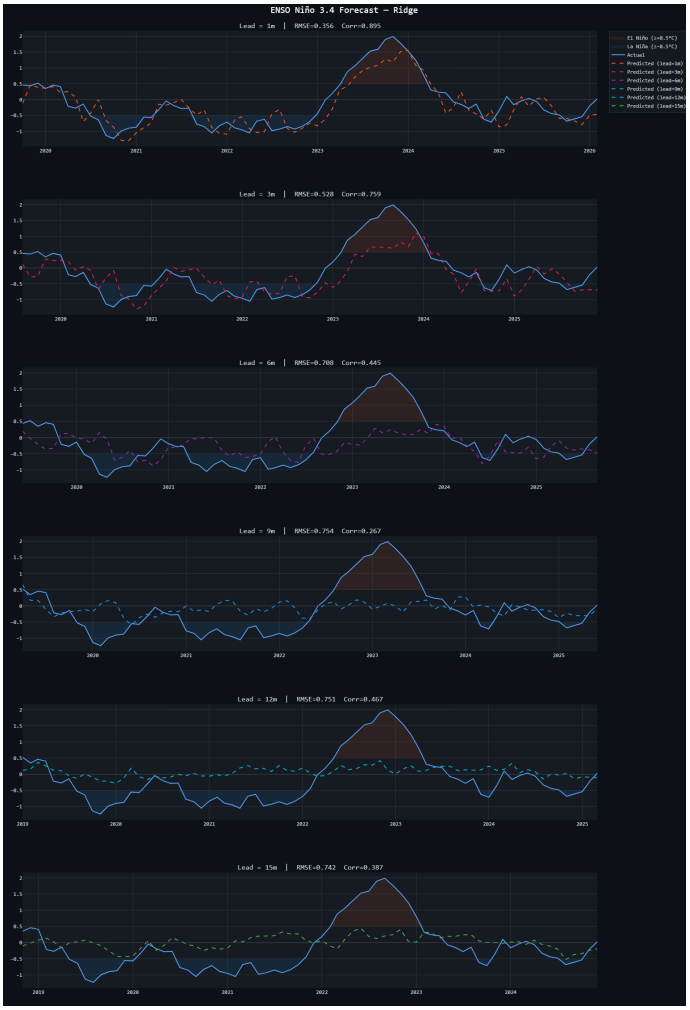

Fig. 7. Ridge Regression: predicted (dashed) vs. observed (solid) Niño 3.4 for all six lead times. El Niño/La Niña periods shaded red/blue.

Fig. 8. LSTM: predicted (dashed) vs. observed (solid) Niño 3.4. Skill is strongest at 1–3-month leads and degrades substantially beyond 6 months.

is because SST anomalies are highly persistent over short periods. But as the forecast lead time becomes larger, the predictive capabilities of all models become worse due to greater uncertainty in ocean-atmospheric processes.

Secondly, among all the models, LSTM model performs better than the other models at longer lead times since it can detect long-range temporal relationships. For instance, its predictive capability holds steady up until 9 months, unlike that of Ridge Regression model, which deteriorates the most rapidly due to its linear structure.

B. Spring Predictability Barrier Effect

The performance is severely hampered in the forecasts that pass the SPB, which confirms the existence of the Spring Predictability Barrier (SPB). In the process of prediction passing through this barrier, SST anomalies diminish, and ocean–atmosphere interactions lessen, thereby increasing the level of uncertainty in forecasts.

Although all models are impacted by the SPB phenomenon, LSTM shows an especially moderate decline in correlations. It can be concluded that the sequence-based models can better detect temporal features during this process than others [5].

C. Comparison with Baseline Forecast

As was expected, the performance of the persistence forecast is quite promising at short lead times due to the high efficiency of this model. After 3 months, however, this model starts to deteriorate very rapidly in comparison with machine learning models [2].

D. Bias-Variance Point of View

Another interpretation of the achieved results is provided by means of the bias-variance dilemma. Since Ridge Regression exhibits high bias and low variance, it underfits the training set and does not learn any non-linear relationships. Random Forest and SVR algorithms exhibit medium values of bias and variance and, therefore, demonstrate moderate performance.

Finally, LSTM shows the best results because of its low bias and sequential structure [10].

E. Practical Considerations

In practical terms, the findings arrived at from this study have great relevance with respect to forecasting applications. Accurate ENSO predictions are very important for agriculture and water resource management, not to mention disaster prevention. It is indeed important that the LSTM networks maintain their effectiveness over a long forecast period [9].

F. Limitations

Nevertheless, some constraints exist with regard to this exciting research. First, the models employed rely primarily on the SST features and not on other atmospheric factors such as wind and pressure indices. Second, neural networks such as LSTM should be properly tuned with sufficient data [24].

G. Conclusion

In conclusion, it is evident that the application of LSTM and machine learning algorithms in predicting ENSO is more accurate than using conventional approaches. Nevertheless, future researches need to explore the challenge of Spring Predictability Barrier and model generalization [2].

VII. Conclusion

In this study, a comprehensive framework is presented, which includes different models in predicting ENSO using machine learning algorithms, where Niño 3.4 is the primary parameter studied. Different models such as ridge regression, support vector regression (SVR), random forest, and long short-term memory (LSTM) were used to predict ENSO occurrence at different lead times ranging from one month to 15 months [18].

From the experiments conducted, the results showed that despite the good prediction results by different models with respect to short lead times (from one to three months), the performance reduces as the lead time increases. This can be attributed to the increased uncertainties arising due to interaction between the atmosphere and ocean as well as complexity of ENSO dynamics. Unlike other models, LSTM performed better in long lead times because of its higher correlation and low error rates when making predictions [16].

Tha is study also highlights some challenges posed by the use of traditional models, particularly ridge regression models, which are very biased and fail to consider the nonlinearity of the ENSO phenomenon. While ensemble models such as random forests and kernel methods like SVR make progress toward achieving balance between bias and variance, their performance deteriorates with increasing lead times [30].

One important finding from the analysis is the existence of the Spring Predictability Barrier (SPB). This has been found to have a huge impact on forecast accuracy regardless of the model used. It is evident that the forecast accuracy reduces sharply when predictions pass through the boreal spring period (March–May), a finding that corroborates existing research literature [10].

Moreover, the comparison of the persistence benchmark model shows that although persistence does quite well for lead times of short duration, it quickly becomes ineffective beyond a three-month period [10]. On the other hand, machine learning algorithms are capable of deriving useful patterns from past data, thus enabling better predictive power in the medium- and long-range [18].

In conclusion, the findings of this study show that machine learning methods can be considered effective in ENSO prediction and have the potential to enhance the performance of standard climate models. Being able to achieve higher predictability compared to traditional methods has substantial real-world application value.

VIII. Future Work

Although the proposed system works well, there are many ways to improve its performance. For instance, incorporating additional parameters such as atmospheric parameters, wind stress, sea level pressure, and outgoing long-wave radiation (OLR) may contribute to better understanding of ENSO phenomena [26].

Moreover, another idea worth exploring is developing hybrid models that will combine the use of physics-based models and machine learning approaches. It can benefit from both modeling methods and enhance its performance.

More sophisticated deep learning approaches like Transformers and attention models can be considered for handling long-term dependencies in climate-related data and detecting complicated patterns. Such techniques proved themselves useful for many sequence modeling problems and could significantly increase prediction accuracy for ENSO events [18].

Furthermore, a wider range of data, both spatially and temporally, can be introduced to improve stability of prediction algorithms and increase their generalizability. The use of transfer and ensemble learning techniques could contribute to achieving this goal [24].

Lastly, future research could be centered around enhancing the interpretability of machine learning algorithms in order to gain insight into the physical mechanisms that govern the variations in ENSO [33].

In summary, this research project has provided an excellent platform upon which the application of machine learning algorithms in seasonal climate forecasting can be explored further.

Acknowledgment

The authors would like to thank the faculty of the Department of Computer Science and Engineering, BMS Institute of Technology and Management, for their guidance and support. The authors also acknowledge the use of NOAA datasets and open-source tools that facilitated this work.

References

[1] M. J. McPhaden, S. E. Zebiak, and M. H. Glantz, "ENSO as an integrating concept in Earth science," *Science*, vol. 314, no. 5806, pp. 1740–1745, Dec. 2006, doi: doi:10.1126/science.1132588.

[2] A. G. Barnston, M. K. Tippett, M. L'Heureux, S. Li, and D. G. DeWitt, "Skill of real-time seasonal ENSO model predictions during 2002–2011: Is our capability increasing?," *Bulletin of the American Meteorological Society*, vol. 93, no. 5, pp. 631–651, May 2012, doi: doi:10.1175/BAMS-D-11-00111.1.

[3] E. K. Schneider, B. Huang, Z. Zhu, D. G. DeWitt, J. L. Kinter III, B. P. Kirtman, and J. Shukla, "Ocean data assimilation, initialization, and prediction of ENSO with a coupled GCM," *Monthly Weather Review*, vol. 127, pp. 1187–1207, 1999, doi: doi:10.1175/1520-0493(1999)127<1187:ODAIAP>2.0.CO;2.

[4] P. J. Webster and S. Yang, "Monsoon and ENSO: Selectively interactive systems," *Quarterly Journal of the Royal Meteorological Society*, vol. 118, no. 507, pp. 877–926, Jul. 1992, doi: doi:10.1002/qj.49711850705.

[5] T. Hastie, R. Tibshirani, and J. Friedman, *The Elements of Statistical Learning: Data Mining, Inference, and Prediction*, 2nd ed., New York, NY, USA: Springer, 2009, doi: doi:10.1007/978-0-387-84858-7.

[6] NOAA Climate Prediction Center, "ENSO Data and Indices," National Oceanic and Atmospheric Administration, [Online]. Available: https://www.cpc.ncep.noaa.gov/data/indices/.

[7] R. J. Hyndman and G. Athanasopoulos, *Forecasting: Principles and Practice*, 3rd ed., Melbourne, Australia: OTexts, 2018, [Online]. Available: https://otexts.com/fpp3/.

[8] D. S. Wilks, *Statistical Methods in the Atmospheric Sciences*, 3rd ed., Amsterdam, Netherlands: Academic Press, 2011, doi: doi:10.1016/C2009-0-00151-1.

[9] S. Hochreiter and J. Schmidhuber, "Long short-term memory," *Neural Computation*, vol. 9, no. 8, pp. 1735–1780, Nov. 1997, doi: doi:10.1162/neco.1997.9.8.1735.

[10] M. Newman, G. A. Vecchi, A. Rosati, and S. G. Yang, "The spring predictability barrier in ENSO forecasts," *Journal of Climate*, vol. 29, no. 24, pp. 8869–8894, Dec. 2016, doi: doi:10.1175/JCLI-D-15-0423.1.

[11] K. E. Trenberth, "The definition of El Niño," *Bulletin of the American Meteorological Society*, vol. 78, no. 12, pp. 2771–2777, Dec. 1997, doi: doi:10.1175/1520-0477(1997)078<2771:TDOENO>2.0.CO;2.

[12] S. Power, T. Casey, C. Folland, A. Colman, and V. Mehta, "Inter-decadal modulation of the impact of ENSO on Australia," *Climate Dynamics*, vol. 15, no. 5, pp. 319–324, May 1999, doi: doi:10.1007/s003820050284.

[13] M. H. Glantz, *Currents of Change: Impacts of El Niño and La Niña on Climate and Society*, 2nd ed., Cambridge, UK: Cambridge University Press, 2001, ISBN: 9780521786720.

[14] S. E. Zebiak and M. A. Cane, "A model El Niño–Southern Oscillation," *Monthly Weather Review*, vol. 115, no. 10, pp. 2262–2278, Oct. 1987, doi: doi:10.1175/1520-0493(1987)115<2262:AMENO>2.0.CO;2.

[15] B. P. Kirtman and P. S. Schopf, "Decadal variability in ENSO predictability and prediction," *Journal of Climate*, vol. 11, no. 11, pp. 2804–2822, Nov. 1998, doi: doi:10.1175/1520-0442(1998)011<2804:DVIEPA>2.0.CO;2.

[16] M. Latif, R. Kleeman, and C. Eckert, "Greenhouse warming, decadal variability, or El Niño? An attempt to understand the anomalous 1990s," *Journal of Climate*, vol. 10, no. 9, pp. 2221–2239, Sep. 1997, doi: doi:10.1175/1520-0442(1997)010<2221:GWDVOE>2.0.CO;2.

[17] F.-F. Jin, "An equatorial ocean recharge paradigm for ENSO. Part I: Conceptual model," *Journal of the Atmospheric Sciences*, vol. 54, no. 7, pp. 811–829, Apr. 1997, doi: doi:10.1175/1520-0469(1997)054<0811:AEORPF>2.0.CO;2.

[18] I. Goodfellow, Y. Bengio, and A. Courville, *Deep Learning*, Cambridge, MA, USA: MIT Press, 2016.

[19] L. Breiman, "Random forests," *Machine Learning*, vol. 45, no. 1, pp. 5–32, Oct. 2001, doi: doi:10.1023/A:1010933404324.

[20] A. J. Smola and B. Schölkopf, "A tutorial on support vector regression," *Statistics and Computing*, vol. 14, no. 3, pp. 199–222, Aug. 2004, doi: doi:10.1023/B:STCO.0000035301.49549.88.

[21] F. Pedregosa, G. Varoquaux, A. Gramfort, V. Michel, B. Thirion, O. Grisel, M. Blondel, P. Prettenhofer, R. Weiss, V. Dubourg, et al., "Scikit-learn: Machine learning in Python," *Journal of Machine Learning Research*, vol. 12, pp. 2825–2830, Oct. 2011.

[22] W. McKinney, "Data structures for statistical computing in Python," in *Proc. 9th Python in Science Conf.*, Austin, TX, USA, 2010, pp. 51–56.

[23] A. Paszke, S. Gross, F. Massa, A. Lerer, J. Bradbury, G. Chanan, T. Killeen, Z. Lin, N. Gimelshein, L. Antiga, et al., "PyTorch: An imperative style, high-performance deep learning library," in *Advances in Neural Information Processing Systems*, vol. 32, 2019.

[24] J. Shukla, "Predictability in the midst of chaos: A scientific basis for climate forecasting," *Science*, vol. 282, no. 5389, pp. 728–731, Oct. 1998, doi: doi:10.1126/science.282.5389.728.

[25] Y. Xue, M. A. Cane, and S. E. Zebiak, "Predictability of a coupled model of ENSO using singular vector analysis," *Climate Dynamics*, vol. 15, pp. 737–750, 2000, doi: doi:10.1007/s003820000075.

[26] N. C. Lau, "Recent climate variability in the Pacific and Indian Ocean regions," *Science*, vol. 271, no. 5253, pp. 1612–1615, Mar. 1996, doi: doi:10.1126/science.271.5253.1612.

[27] C. Penland and P. D. Sardeshmukh, "The optimal growth of tropical sea surface temperature anomalies," *Journal of Climate*, vol. 8, no. 8, pp. 1999–2024, Aug. 1995, doi: doi:10.1175/1520-0442(1995)008<1999:TOGOTS>2.0.CO;2.

[28] D. Lartey Quayesam, J. Abugre Akubire, and O. A. G. Darkwah, "A comparison of machine learning algorithms for predicting sea surface temperature in the Great Barrier Reef region," *arXiv preprint arXiv:2411.15202*, 2024. [Online]. Available: https://arxiv.org/abs/2411.15202.

[29] T. Chen and C. Guestrin, "XGBoost: A scalable tree boosting system," in *Proc. 22nd ACM SIGKDD*, 2016, pp. 785–794, doi: doi:10.1145/2939672.2939785.

[30] Y.-G. Ham, J.-H. Kim, and J.-J. Luo, "Deep learning for multi-year ENSO forecasts," *Nature*, vol. 573, no. 7775, pp. 568–572, Sep. 2019, doi: doi:10.1038/s41586-019-1559-7.

[31] H. Wang, S. Hu, and X. Li, "An interpretable deep learning ENSO forecasting model," *Ocean-Land-Atmosphere Research*, vol. 2, 2023, doi: doi:10.34133/olar.0012.

[32] M. Saha and R. S. Nanjundiah, "Prediction of ENSO indices using deep learning," *Meteorological Applications*, vol. 27, no. 1, 2020, doi: doi:10.1002/met.1826.

[33] Y. Gan et al., "Explainable ENSO forecasting using deep learning," *arXiv preprint arXiv:2601.02050*, 2026. [Online]. Available: https://arxiv.org/abs/2601.02050.

[34] J. Feng et al., "Achieving explainable ENSO prediction using small data training," *Geophysical Research Letters*, vol. 53, 2026, doi: doi:10.1029/2025GL117573.

[35] J. Schloer et al., "A hybrid deep-learning model for ENSO in the low-data regime," *arXiv preprint arXiv:2412.03743*, 2025. [Online]. Available: https://arxiv.org/abs/2412.03743.